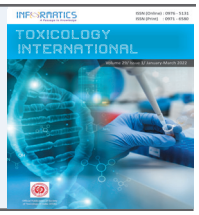
Toxicology International, *29(1) : 1-14; 2022. DOI: 10.18311/ti/2022/v29i1/24000*

Online ISSN : 0976-5131; Print ISSN : 0971-6580

Toxicology International

Contents available at: www.informaticsjournals.com/index.php/toxi



Toxicological Sequelae of Pesticide Combinations Exposure in Buffalo Mesenchymal Stem Cells under *In Vitro*

H. Singh[1], M. K. Lonare[1]*, M. Sharma[2], R. Udheya[3], S. Singla[1] and V. K. Dumka[1]

[1]Department of Veterinary Pharmacology and Toxicology, Guru Angad Dev Veterinary and Animal Sciences University, Ludhiana – 141004, Punjab, India; drmilind12@rediffmail.com
[2]Department of Veterinary Physiology and Biochemistry, Guru Angad Dev Veterinary and Animal Sciences University, Ludhiana – 141004, Punjab, India
[3]Department of Veterinary Surgery and Radiology, Guru Angad Dev Veterinary and Animal Sciences University, Ludhiana – 141004, Punjab, India

ARTICLE INFO

KEYWORDS: Carbendazim, Imidacloprid, Mesenchymal Stem Cells, Mitochondrial Transmemberane Potential, Reactive Oxygen Species (ROS), Senescence

ARTICLE HISTORY
Received: 30.07.2019
Revised: 14.08.2019
Accepted: 10-06-2021

Abstract

The presence of one or more pesticides in a variety of mediums is responsible for their indirect toxicological events leading to cell senescence. In the present investigation, the endeavor was made to see the effect of pesticides Car-Benda-Zim (CBZ) and IMIdacloprid (IMI) alone and in combination with bone marrow-derived Mesenchymal Stem Cells (bMSCs) of buffalo origin. Isolated and cultured bMSCs were exposed to CBZ and IMI alone and in combinations at lower doses. Cells were observed for alterations in cell morphology, oxidative stress, mitochondrial damage and cellular senescence. bMSCs characterized for stem cell surface markers and found to be positive for AP, CD73 and OCT4. bMSCs exposed to IC25, IC12.5 and IC6.25 CBZ and IMI alone and combinations of IC12.5 and IC6.25 of CBZ and IMI. Results revealed significant reduction ($p \leq 0.05$) in cell viability noticed on microscopic examination along with loss of normal cell morphology and increased in Reactive Oxygen Species (ROS) positive cells, cells with loss of $\Delta\Psi m$ and number of senescent cells in CBZ and IMI treated groups. Lower dose combination groups showed elevated effects when compared with higher dose alone treated groups and control groups. Present findings suggest that CBZ and IMI induced cytotoxicity in bMSCs mediated via ROS production, altered $\Delta\Psi m$ leading to the cell damage and predisposing senescence process. Moreover, the co-existence of CBZ and IMI in a medium has a considerably more toxic effect than their individual effect.

*Author for correspondence

1. Introduction

The application of pesticides in modern agriculture practices has been increased many-fold to control pest infestation and increase food production and prevent production losses. In the category of pesticide, insecticides and fungicides are a major one, whose use is highest in agriculture followed by herbicides and rodenticides. Application one or more chemical pesticides at a time more than recommended level is common practice under field conditions responsible for residual accumulation in food commodities such as feed and fodder more than NOEL and MRL level. Long-term consumption of low levels of pesticides through foodstuff compromises the health of humans and animals[1]. Car-Benda-Zim (CBZ) is a broad-spectrum fungicide belongs to the benzimidazole group. It plays a very vital role in the control of fungal infestation in plants. CBZ is categorized under the category of endocrine disruptor even though use has not been stopped but increased by many folds. Many other adverse effects associated with the use of CBZ in the living system have been published in recent years[2]. It has a toxic effect on the testis and ovaries and alters hormonal regulation, impairs sexual maturity and interferes in foetal development[3]. Hence the use of CBZ has been restricted in many countries recently. In the category of insecticide, IMIdacloprid (IMI) belongs to the neonicotinoid group. IMI is a principal compound of this group known for its worldwide application. It has agonistic activity in insects, which acts on nAChRs but it has a lower affinity for mammal nAChRs compared with insects[4]. Hence, use as endo-ectoparasiticide in animals and garden insect-pest management in agriculture has been increased in the last two decades[5]. Many researchers reported long-term exposure to IMI may be responsible for neurotoxicity, reproductive toxicity, and immunotoxicity in mammals[6]. It may cause damage to the heart, liver, kidney, and other vital organs in non-targeted animal species[5,7].

Pesticides are the common eco-toxicant that may be responsible for adverse effects on every component of the ecosystem. Millions of people and other non-target organisms are victims of their exposure. The effects are associated with the application of many pesticides for pest management. Thus, animals and humans are mostly exposed to more than one eco-toxicant is a reality through the exposure of persistent residual levels from a variety of mediums. These pesticides interact in the body in many ways depending on their chemical nature, presence of other chemicals, animal species, the target organ, affinity to the receptor site, and ultimately individual body composition[8]. The term drug interaction refers to a physiological situation where two or more drugs influence the physio-pharmacological effect of each other[4]. They may interact at toxicokinetic, toxicodynamic levels, may involve other metabolic processes and/or molecular targets of individuals. These complications may lead to unpredictable toxic effects[9].

In view of the above facts, there is a lot of scope in investigating the interactive effect of commonly used pesticides belonging to different categories in different target species. In particular, bovines are used as a target species to evaluate the toxic effect of pesticides. Hence, bone marrow-derived Mesenchymal Stem Cells (bMSCs) of buffalo origin have been adopted as *in vitro* test systems to evaluate the effect of fungicide and insecticide alone and co-existence.

2. Materials and Methods

2.1 Chemicals and Reagents

Carbendazim (97 %) was procured from Sigma Aldrich, USA. while imidacloprid (94 %) procured from M/s Gharda Chemicals, Pvt. Ltd. Mumbai. All other chemicals were of analytical grade and plastic wares for cell culture obtained from established firms (Sigma, Bangalore-Genei, Himedia, Merck, SD fine chemicals, Span Diagnostics and ERBA Diagnostics Pvt. Ltd).

A stock solution of I M (2 M; 510.2 g L^{-1}) and CBZ (0.5 M; 95.6 g L^{-1}) was prepared in DMSO. The complete growth medium (CGM) was prepared in Dulbecco's Modified Eagle's Medium (DMEM) with the addition of 15 % FBS and antibiotics. Prepared Phosphate Buffer Saline (PBS) of pH 7.4 autoclaved and stored at 4°C for routine use.

2.2 Mesenchymal Stem Cell Culture and Expansion

Bone marrow samples were aspirated from iliac crest of the pelvis immediately after stunning the buffalo calves in slaughter house under the sterile condition with the help of a sterile Jamshidi needle (11 G) in 20-ml syringes containing 250 units of heparin. A mixed population of

stem cells was isolated with density gradient method using Histopaque-1077 (1:1 ratio) by centrifuging at 2500 rpm for 30 minutes at room temperature. The visible buffy coat consisted of mix population of cells (lymphocytes and stem cells) was carefully transferred to another centrifuge vial and washed with PBS by centrifugation at 800 rpm for 10 minutes. The resultant pellet was mixed with RBC lysis buffer at room temperature for 5 min. Finally, three washing with PBS was given to the cells, and the pellet was resuspended in CGM for incubation in an incubator provided with 5 % CO_2 at 37 ^{0}C temperature.

2.3 Mesenchymal Stem Cell Characterization

2.3.1 Alkaline Phosphatase Staining

Alkaline Phosphatase (AP) staining in bMSCs was done after 3rd passage. Approximately 1.5X10^5 bMSCs per mililitre of CGM were seeded into six well culture flasks. Cells when attended 70 % of confluency were fixed with 4 % paraformaldehyde for 10 min at 37 °C in the incubator. Finally, bMSCs were incubated AP stain (25 mM Tris-HCl and 150 mM NaCl containing 8 mM $MgCl_2$, 0.4 mg/ml Naphthol AS-MX Phosphate and 1 mg/ml FastRed TR salt for 1 hr at 37 °C). Finally, cells were visualized under a bright field.

2.3.2 Immunohistochemistry

When cells attended approximately 70 % confluency cells were fixed 4 % paraformaldehyde solution and washed as mentioned in an earlier section. Non-specific primary antibody bindings were blocked using donkey serum (1:10 dilution in PBS) by incubating at 37 °C for 5 minutes. bMSCs were initially incubated with CD73 and OCT4 primary antibodies followed by secondary antibodies conjugated with FITC and/or TexasRed for 1 hr at 37°C. Finally, cells were visualized under a fluorescence microscope.

2.4 Population Doubling Time (PDT)

When bMSCs reached >80 % confluency, trypsinized with 0.25 % Trypsin Phosphate Versene Glucose (TPVG) to obtained single cell suspension. Finally, the cell pellet was resuspended in 1 ml CGM. Cell number and cell viability were determined by the trypan blue dye exclusion method. Cells with viability of more than 90-95 % were used in the experiment. The cell concentration was adjusted 1x10^5 cells/mL of culture medium.

Population Doubling Time (PDT) was estimated by the Neutral Red Uptake (NRU) assay[10] in cells from third passaged. Change in absorbance was recorded and the number of cells was counted with the standard published formula[11].

2.5 Determination of Inhibitory Concentration (IC_{50})

CBZ concentrations ranging from 0.254 µM to 5 mM and IMI concentrations ranging from 0.0106 µM to 400 mM were prepared in CGM by serial dilution from the stock solution. Cell viability assay/MTT assay was performed as per the procedure described in the published article[12] and IC_{50} concentration was calculated. A log dose-response curve was plotted for determination of IC_{50} as per the standard formula (% of cell survival = [Absorbance test / Absorbance control] x 100; IC_{50}= 100 - % of cell survival).

2.6 Experimental Design

Based on the IC50 value of CBZ and IMI, the three individual concentrations were selected IC_{25}, $IC_{12.5}$ and $IC_{6.25}$ for alone treatment while combinational effect, $IC_{12.5}$ and $IC_{6.25}$ concentration were used (Table 1). All experiments were performed in triplicate (n=3) with three replicates each. The average value of replicates was taken as one.

2.6.1 Cell Morphology

Cytotoxic effects of CBZ and IMI alone and combinations were assessed in bMSC's and cellular morphology was scored by visualizing under an inverted microscope based on their degrees of cellular changes. Visual observation, codes in the description of cell culture changes were used as described in an earlier publication of our laboratory[10].

2.6.2 Measurement of Reactive Oxygen Species (ROS) and ΔΨm

Cells were trypsinized and were seeded in 96 well culture plates with cell density 1.5x10^5 cells/ml of CGM. 12 hours cell attachment treated with CBZ and IMI for 3 hrs. A stock solution of 2 mM DCFHDA (working solution

Table 1. Experimental design showing the treatment groups of bMSCs with CBZ and IMI alone and in combinations

Group	Treatment	Dose
I	Control	-
II	DMSO	1%
III	CBZ-I	2.25 µM/ml
IV	CBZ-II	4.49 µM/ml
V	CBZ-III	8.98 µM/ml
VI	IMI-I	805 µM/ml
VII	IMI- II	1.61 mM/ml
VIII	IMI- III	3.22 mM/ml
IX	CBZ-I + IMI- I	2.25 µM/ml + 805 µM/ml
X	CBZ-I + IMI- II	2.25 µM/ml + 1.61 mM/ml
XI	CBZ-II + IMI- I	4.49 µM/ml + 805 µM/ml
XII	CBZ- II + IMI- II	4.49 µM/ml + 1.61 mM/ml

Where; DMSO: dimethylsulfoxide; CBZ: carbendazim; IMI: imidacloprid.

20 µM) and 1 mM $DiOC_6$ (working solution 10 µM) was prepared and used for the study. 2,7-dichlorofluorescin diacetate (DcFHDA) assay was used to estimate total ROS (hydroxyl, peroxyl and other ROS) production within the cell according to the standard method[13] and 3,3- dihexyloxacarbocyanine iodide [$DiOC_6(3)$] was used to estimate the loss of $\Delta\Psi m$ as described by Salmon[14].

2.6.3 Cell Senescence Analysis

bMSCs exposed to CBZ and IMI were used for the detection of senescence changes using a cell senescence detection kit. Cells stained blue showed senescence. Healthy cells were remained unstained and appeared red after counter-staining with Neutral Red Dye (0.33 % gm) for 5 min and washed with DPBS.

2.7 Statistical Analysis

The data generated in this study compiled and employing one way analysis of variance (ANOVA) with Duncan multiple comparisons as post hoc test using GraphPad Prism data analysis software. All the data were expressed as Mean ± SEM. A p value of <0.05 was considered statistically significant.

3. Results

3.1 Establishment of bMSCs Culture and Cell Morphology

Bone marrow mesenchymal stem cells were isolated based on their plastic adherence property. These cells during primary culture showed round, non-

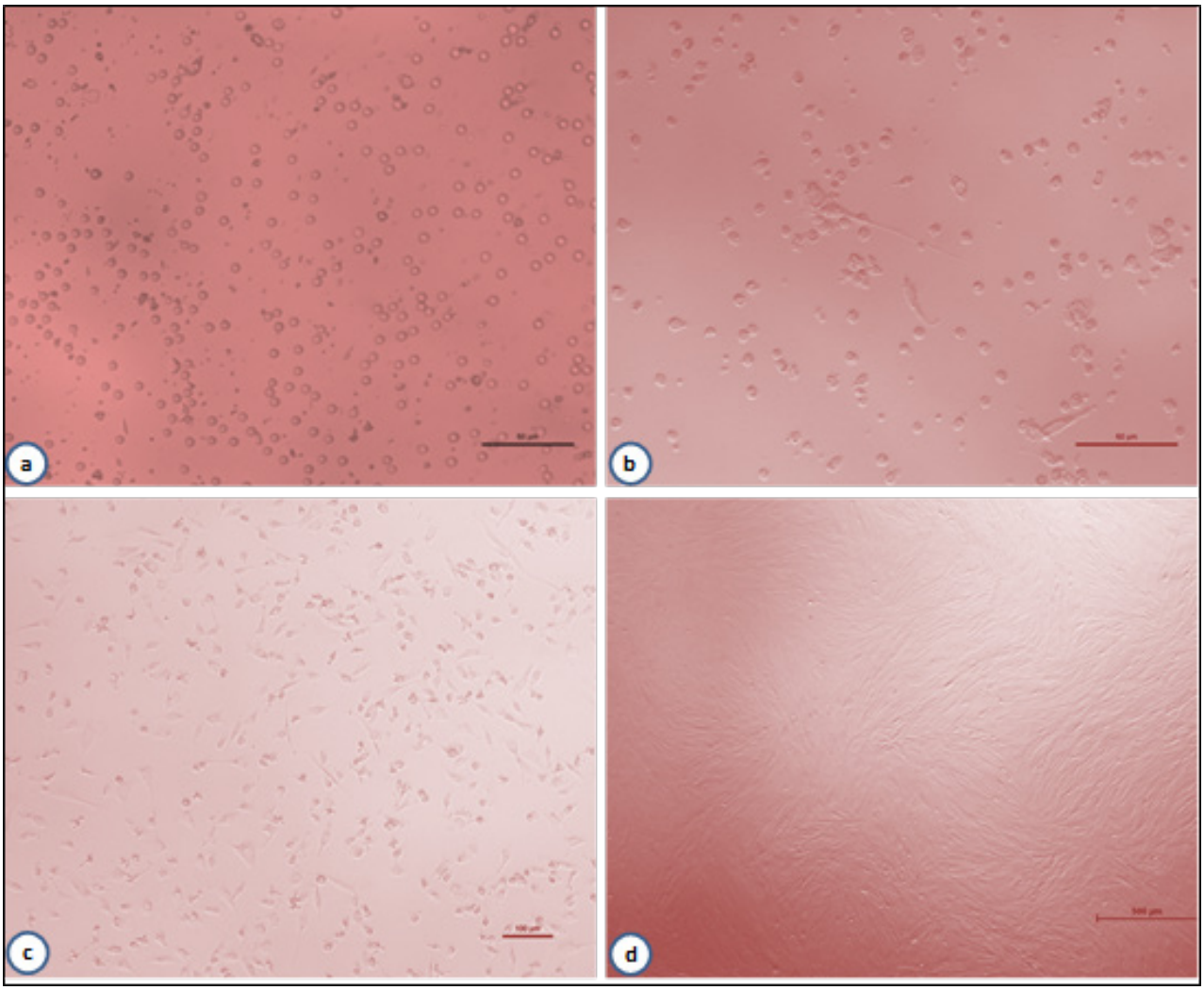


Figure 1. Isolation and culture development of bone marrow derived buffalo mesenchymal stem cells at different time and passages. **(a).** Day **(b).** v: day 3; **(c).** day 15; **(d).** fully confluent monolayer with uniformed cell population at 3 passage. (Original magnification: a & b: X40; c: X20; d:X4).

fibroblastic morphology on day 0 of culturing (Figure 1a). Mesenchymal stem cells attached to cell culture flask from 12 hrs to 72 hours of seeding, consisting of round and spindle-shaped cells (Figure 1b). Adherent cells grew-up as fibroblast-like structures and formed symmetric colonies on day 15 (Figure 1c). The confluent monolayer was obtained on day 28. Uniformed bMSCs populations were received after the third passage (Figure 1d).

3.2 Stem Cell Characterization

The alkaline phosphatase activity was detected positive in bMSCs and cells appeared red under bright field (Figure 2). AP positive cells were indicative of a healthy and actively growing state, expressed phenotypically and undifferentiated condition. The bone marrow-derived MSCs showed positive expression of cell surface markers CD73 and OCT4 as revealed by green and red fluorescence all over the cells, respectively (Figure 3).

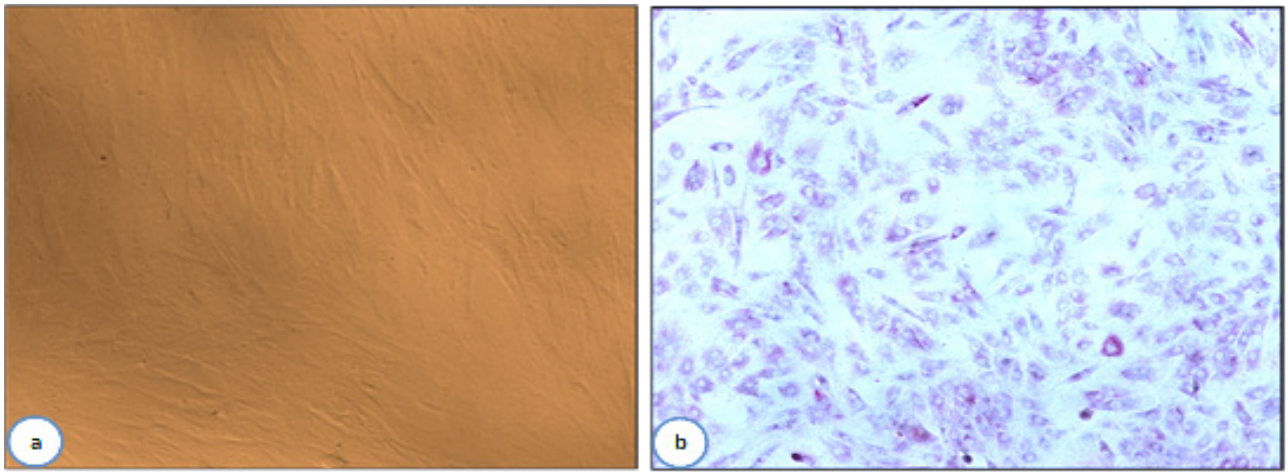


Figure 2. Representative photomicrographs showing alkaline phosphatase staining in bMSCs under inverted microscope **(a).** before staining, and **(b).** after staining.

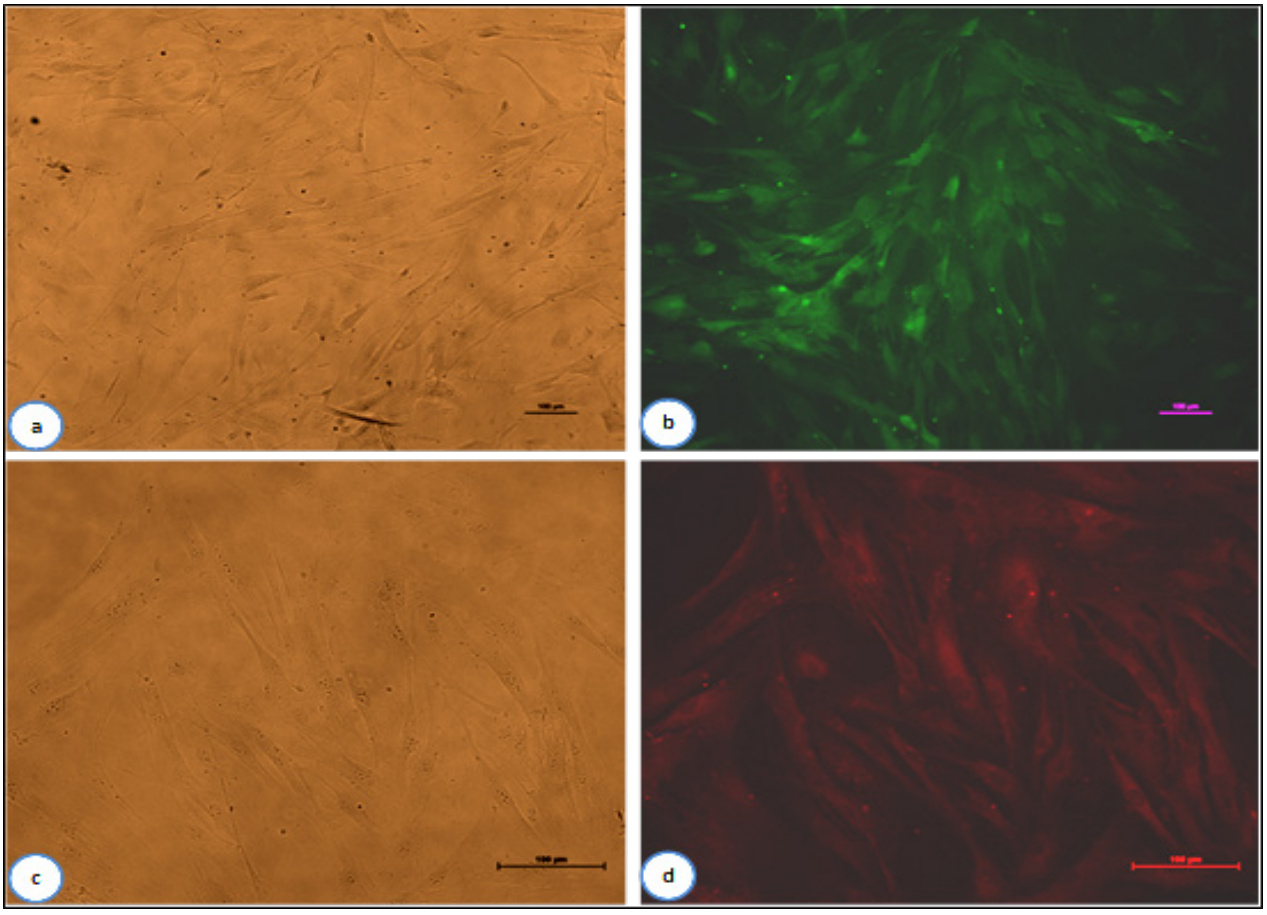


Figure 3. Representative photomicrographs immunofluorescent staining of buffalo bMSCs for localization of CD73 **(a&b),** and OCT4 **(c&d)** with FITC or Texas Red-conjugated secondary antibodies, respectively. (Original magnification: A - F: X10; a&c: under bright field; b&d: under fluorescent).

Polyclonal antibody specific to MSCs cell surface antigens CD73 and OCT4 were used to characterize the MSCs progenitor and pluripotency.

3.3 PDT and IC_{50} Concentration

The average Population Doubling Time (PDT) of bMSCs was found to be 39.21 hrs, with a variation of 33.61 hrs to 43.94 hrs (Table 2). Further, IC_{50} of CBZ was found to be 17.97 µM, while, and IMI was found to be 6.45 mM after 48 hrs of post-exposure (Figure 4). Further, IC_{25}, $IC_{12.5}$ and $IC_{6.25}$ were calculated to be 8.98, 4.49, 2.25 µM for CBZ and 3.22, 1.61, 0.81 mM for IMI.

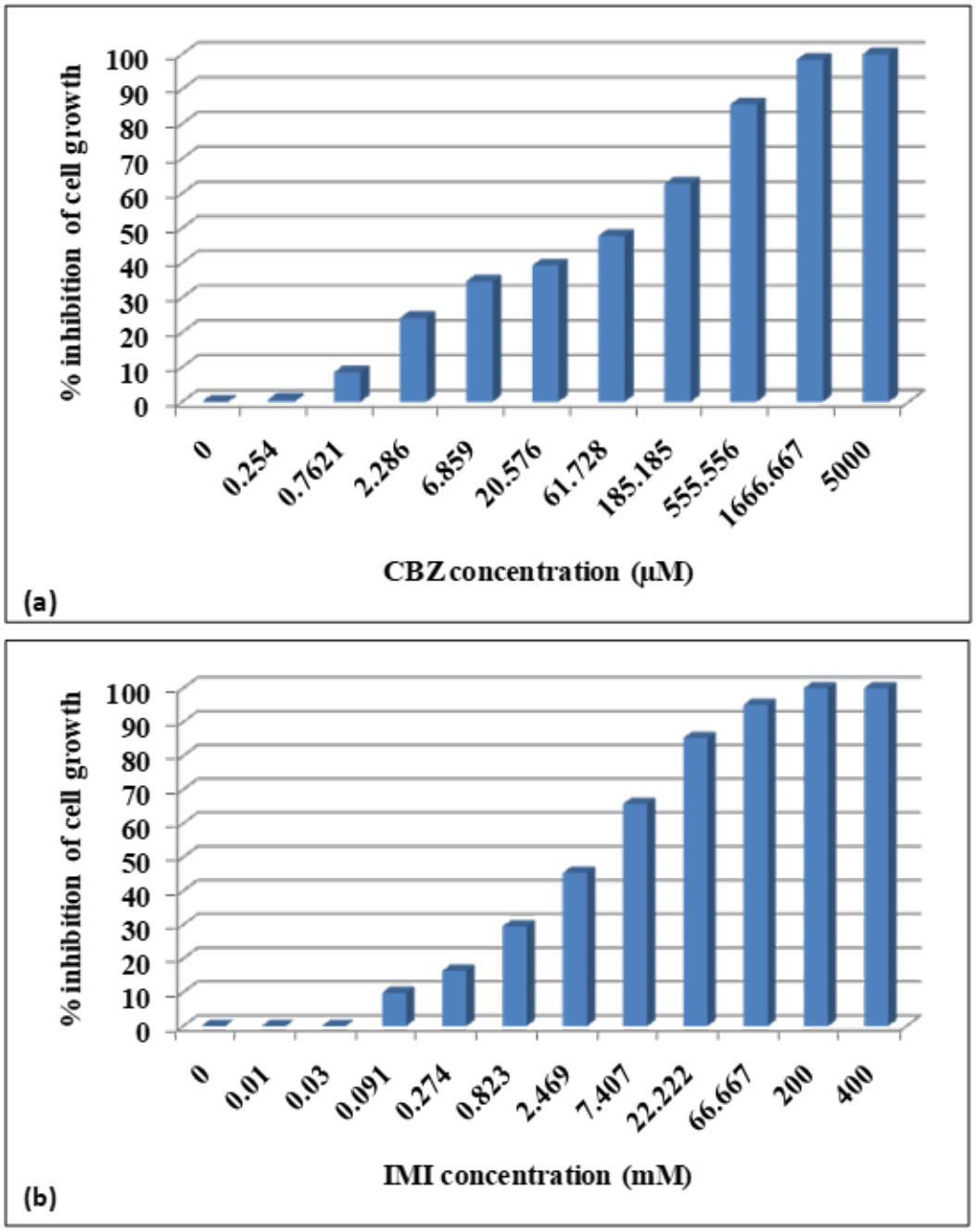


Figure 4. Effect of CBZ and IMI on MSCs derived from buffalo bone marrow proliferation inhibition in 48 hrs post exposure.

Table 2. Population doubling time of MSCs derived from buffalo bone marrow

Sample No.	Initial OD	Initial cell number (X_b)	Final OD	Final cell number (X_e)	Xe/X_b	Log (X_e/ X_b)	Log_2	PDT (hrs)
1.	0.1193	21000	0.3257	58879.18	2.804	0.4477	0.301	33.61
2.	0.1312	21000	0.2842	51376.92	2.447	0.3885	0.301	38.73
3.	0.1224	21000	0.2911	52624.28	2.506	0.3989	0.301	37.72
4.	0.1429	21000	0.2556	46206.69	2.200	0.3425	0.301	43.94
5.	0.1099	21000	0.2708	48954.50	2.331	0.3676	0.301	40.94
6.	0.1361	21000	0.2811	50816.51	2.420	0.3837	0.301	39.22
7.	0.1392	21000	0.2810	50798.43	2.419	0.3836	0.301	39.23
8.	0.1226	21000	0.2776	50183.79	2.390	0.3783	0.301	39.78
9.	0.1557	21000	0.2837	51286.53	2.442	0.3877	0.301	38.81
10.	0.1483	21000	0.2761	49912.62	2.377	0.3759	0.301	40.04
Average PDT								39.20 hrs

3.4 Cytotoxic Effect and Cell Morphology

The normal confluent fibroblast-like structure with elongated and flat morphology was observed in cells from the control group. Varying degrees of morphological changes were observed in CBZ and IMI, alone and in combinations treated groups (Figure 5). Morphological

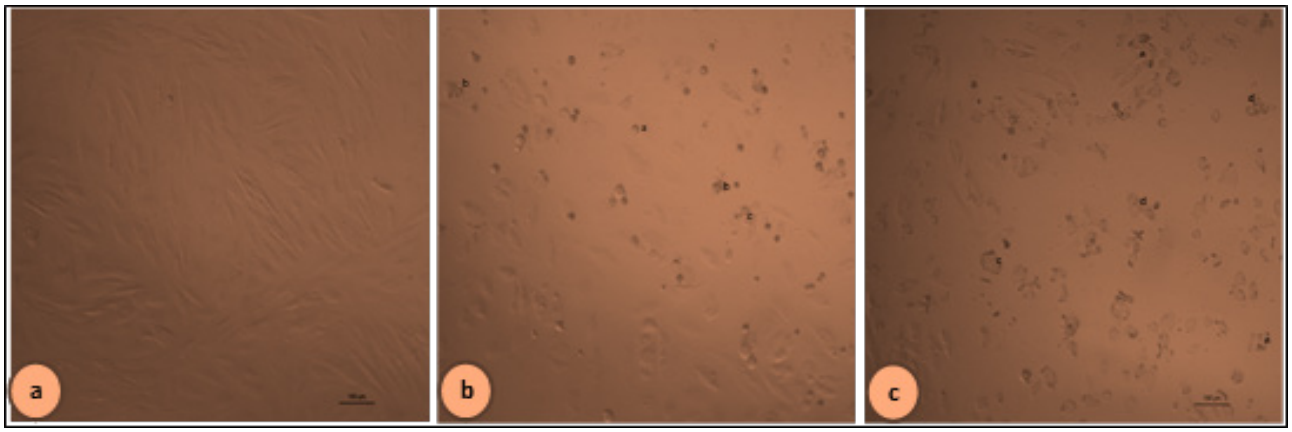


Figure 5. Representative photomicrographs showing bMSCs under inverted microscope after 48 hrs post exposure with CBZ and IMI alone and in-combinations. **(a)** Showing normal cell morphology of bMSCs in the control group. **(b & c)** bMSCs showing varying degree of cellular damage after exposure to pesticides (cell shrinkage; chromatin condensation; intracytoplasmic granulation and rounding of dead cells). (Original magnification: a-c: X10).

Table 3. Scoring of toxicomorphological changes in bMSC's after 48hrs post exposure to CBZ and IMI alone or in combinations.

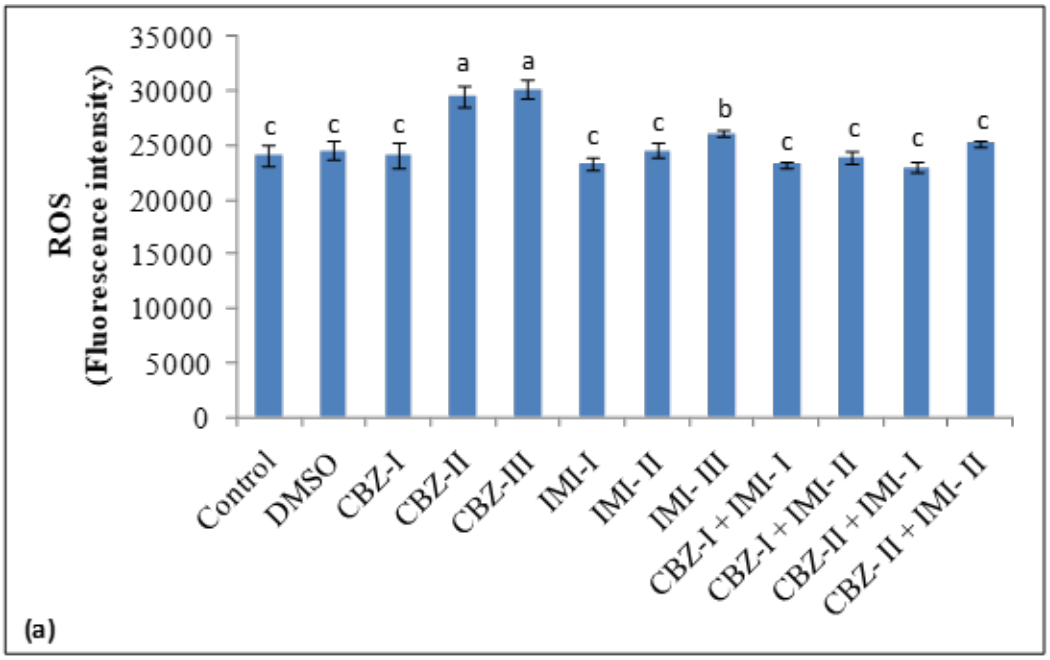
Morphological features	Treatment Groups											
	I	II	III	IV	V	VI	VII	VIII	IX	X	XI	XII
Cellular swelling	1	1	2	3	4	2	3	5	1	1	2	4
Chromatin condensation	1	2	2	4	5	1	2	4	1	2	3	5
Nuclear fragmentation	1	1	1	3	4	1	3	4	2	2	3	5
Loss of plasma membrane	1	1	2	3	4	2	3	3	1	1	2	4
Release of cytoplasmic content	1	1	2	2	3	1	1	4	1	1	1	4

1: Normal morphology; 2: Low level changes; 3: Moderate level changes; 4: High level changes, and 5: Very high level changes.

changes were in dose-dependent manner, comparatively higher in high doses of CBZ and IMI alone and combined dose of CBZ-II+IMI-II as compared to low and medium alone CBZ and IMI groups. Changes in treatment groups were reflected in the form of cells detachment from the surface and dispersed in the culture medium, showing a rounding/spherical morphology. CBZ and IMI resulted in progressive alterations of cellular morphology such as cytoplasm vacuolization, shrinkage, the formation of blebs on the cell surface, reduction of nuclear sizes, which often displayed diverse degrees of chromatin condensation and cell membrane destruction along with dissolution in higher doses. These changes have been scored and presented in Table 3.

3.5 Effect on ROS and MTP/ΔΨm

Early changes in ROS production were measured after 3 hrs of exposure to CBZ and IMI (Figure 6a). Significantly



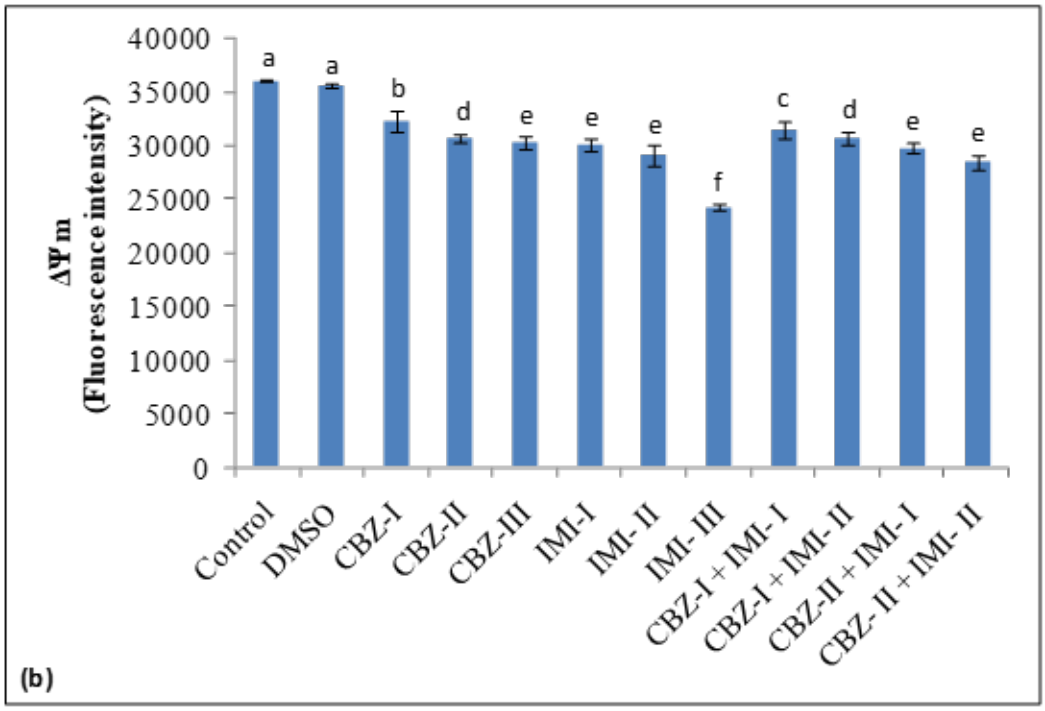


Figure 6. Effect of CBZ and IMI in alone or in combinations on ROS production and loss of ΔΨm in bMSCs with 3 hrs post exposure.

higher ($p \leq 0.05$) fluorescence intensity was noticed at doses CBZ and IMI alone treated groups as compared to control groups. Dose dependant increase in fluorescence intensity was observed in both CBZ and IMI alone treated groups. Co-treated groups did not show significant changes ($p \geq 0.05$) in fluorescence intensity as compared to the control group.

Alteration in ΔΨm in bMSCs was measured after 3 hrs exposure to CBZ and IMI alone and in-combinations (Figure 6b). Significantly lower ($p \leq 0.05$) fluorescence intensity was measured at doses CBZ and IMI alone treated groups when compared with the control group. Significant decrease ($p \leq 0.05$) in fluorescence intensity in dose-dependent in CBZ treated groups and non-significant ($p \geq 0.05$) decrease in IMI treated groups were measured. Co-treated groups showed a significant decrease ($p \leq 0.05$) in fluorescence intensity as compared to the control group but comparable to alone treated groups.

3.6 Effect on Cell Senescence

bMSCs when exposed to the different concentrations of CBZ and IMI caused an increase in the senescent process in dose dependant manner (Figure 7). In co-treatment groups showed a similar pattern of cell senescence. Cells positive for senescence showed blue coloration indicating an increase in beta-galactosidase activity.

4. Discussion

Typical large fibroblast-like morphology is a common feature of MSCs in many species of animals. There is a wide variation in shape from polygonal to spindle-shaped cells even within the same species. Fibroblast-like morphological characteristics of bMSCs on subsequent culturing have been reported from cells isolated from humans and buffalo[11,12,15]. These mesenchymal stem cells essentially need to be confirmedfor progenitor and pluripotency by using surface markers such as CD73, CD44, CD90, and CD105 as per the International Society for Cytotherapy[16,17]. In the present study, we demonstrated that the bMSCs of buffalo origin showed typical morphological characteristics along with positive for alkaline phosphatase activity indicative of metabolically active bMSCs and positive for stemness by expressing CD73 and OCT4. Similarly, caprine/ bovine

MSCs derived from fetal amniotic adnexa were reported to be positive for AP activity and expression of CD73 and OCT4[11,12]. PDT values which vary from 36.66 hrs to 38.63 hrs for bMSCs buffalo, porcine, caprine, canine and human have been reported[11,12,18,19]. These PDT values indicate a very closer proximation to the PTD value of the present work. While Rentschetal[20] was reported a considerably higher PDT value of 50 hrs in sheep.

IC_{50} value of IMI (mM) was found to be very high as compared to the IC_{50} value of CBZ (µM) in the present study. These values indicate reverse feedback of *in vivo* LD_{50} values. IMI is metabolized by two important enzymes in the liver, one is oxidatively metabolized by cytochrome P450 enzymes (CYP3A4) and the other is liver cytosol (aldehyde oxidase) to the C=N-NO_2 (nitroguanidine) moiety. It reduced to C=N-NO (nitrosoguanidine) and C=N-NH2 (aminoguanidine) and cleaved to C=NH (guanidine) and C=O (urea) derivative[21]. The nitrosoguanidine (C=N-NO) metabolite of IMI has moderate to high insecticidal activity through nAChR, whereas, the guanidine (C=NH) metabolite is highly active against mammalian nAChR but inactive against insect nAChR. These metabolites are more toxic to the mammalian system rather than the parent compound IMI[22]. The absence of a metabolic enzyme system under *in vitro* conditions might be responsible for the higher value of IMI required producing its toxic effect on bMSCs. Another possibility is that IMI produced its toxicity through the binding on nAChR, which are mostly present in neuronal tissues/cells than any other cells. To produce its toxic effect by other mechanisms may require more concentration, which was reflected by a higher (IC_{50}) value of IMI than CBZ compared to the *in vivo* toxicity values[23]. Moreover, CBZ interferes' the microtubule formation, binds to tubulin-colchicine binding sites, cell cycle arrest and may produce a toxic effect eukaryotic system including mammalian cells.

ROS generation resulting from oxidative stress in the cell is generally due to failure of intracellular antioxidant defense systems to neutralize the excess of ROS or the inability of the cell to repair the oxidative damage caused by toxicological agents. The generation of ROS is involved in the toxicological interventions of pesticides that cause DNA damage and DNA fragmentation. It has been reported that the presence of cypermethrin and/or chlorpyrifos pesticides in the body gives rise to ROS production and DNA damage[6,24]. Exposure to low doses of pesticides is capable of inducing ROS generation which may become the leading cause of genotoxicity and apoptosis[24]. Higher ROS production was noticed when exposed to the combination of pesticides as compared towhen they were used alone in the present study. Similar to the finding of the present study, the synergistic effect of the combination on ROS production and cell cytotoxicity has been reported on human keratinocyte cell line when exposed to the alpha-hexachlorocyclohexane, parathion and carbofuran mixture when compared to the alone treatment[25].

An apoptosis-inducing drug such as pentamidine (dicationic drug) is responsible for alteration in the ΔΨm. Many chemicals are responsible for the induction of loss of ΔΨm which may lead to apoptosis even in parasites[26,27]. Cell condensation and disruption of kinetoplast of DNA core and collapse of ΔΨm were responsible for cell death[28]. Cells exposed to toxicants resulted in a decrease in fluorescence intensity due to loss of ΔΨm can be directly used as an indicator of cytotoxicity. Another possibility is that when there is damage to the cell membrane due to exposure to toxicants, cytochrome *c*get leaked from the mitochondrial intermembrane space into the cytosol which results in rapid dissipation of ΔΨm and is known to be a major cause for loss of ΔΨm. As cytochrome *c* promotes the pumping of protons into the mitochondrial intermembrane by shuttling electrons from Complex III to Complex IV and is essential for producing ΔΨm. MTP may influence the process of apoptosis and cell death[29]. This explanation also supports the findings of the present study correlating with ROS production, loss of ΔΨm, and cytotoxic damage. Pesticides exert their action through oxidative phosphorylation as a primary and mitochondrial membrane as a secondary target. Generation of ROS, reactive nitrogen species impair oxidative phosphorylation and cause alteration in mitochondrial respirationwhich isresponsible for apoptosis and necrosis[30,31].

Cellular senescence is a complex stress response process whereby cells irreversibly lost the capacity to proliferate, and become resistant to growth-promoting stimuli accompanied by numerous changes in gene expression[32,33]. Cells include endogenous germ line and somatic stem cells, in addition to embryonic or induced pluripotent stem cells developed under controlled *in vitro* conditions may undergo early senescence with a varying degree in response to stress conditions[33]. The number of

senescent cells increases with age, but senescence may also play an important role during the development and healing process[34]. Free radicals can damage proteins, lipids, and DNA, while, glycation mainly damages proteins. Damaged proteins and lipids accumulate in lysosomes as lipofuscin. Chemical damage to structural proteins can lead to loss of function or damage to enzymes which reduces cellular functionality. Lipid peroxidation of the inner mitochondrial membrane reduces the electric potential and the ability to generate energy and accelerate aging by defective DNA repair enzymes[35,36] and predispose the senescent process. Toxins and toxicants induce amnion cell senescence via a mechanism involving ROS and DNA damage. Activation of ASK1, P-p38 MAPK, and p19Arf correlated with the number of SAB-gal expressing cells after cigarette toxin treatment has been reported[37]. These reports support the findings of the present study as an increase in the level of ROS, loss of MPT, that responsible for exogenous agents that induced cellular senescence.

5. Conclusion

Present findings confirm that CBZ and IMI induced cytotoxicity in bMSCs mediated via ROS production, ΔΨm responsible for cellular damage, apoptosis, and senescence under isolated conditions, CBZ has apredominant cytotoxic effect on bMSCs than that of the IMI. However, their co-existence of CBZ and IMI in a medium even at a lower dose in concentrationhas an additive or synergistic effect on cellular events that lead to exaggerated toxic effectsequivalent to the higher dosesof CBZ and IMI alone.

6. Acknowledgments

The authors are thankful to the Dean Post Graduate Studies and the Director of Research, Guru Angad Dev Veterinary and Animal Sciences University Ludhiana, Punjab, India, for providing research facilities to carry out research work. The author likes to acknowledge all the peoples who have directly or indirectly been involved in the completion of this research work.

7. Declaration of Conflicting Interests

The author(s) declared no potential conflicts of interest with respect to the research, authorship, and/or publication of this article.

8. References

1. Damalas CA, Koutroubas SD. Farmers' Training on pesticide use is associated with elevated safety behavior. Toxics. 2017; 5(3):19. https://doi.org/10.3390/toxics5030019. PMID: 29051451; PMCID: PMC5634698.
2. Patil N, Lonare M, Sharma M, Lalhriatpuia P, Saini S, Rampal S. Hemato-biochemical alterations mediated by carbendazim exposure and protective effect of quercetin in male rats. Toxicol Int. 2018; 25(1):1-12. https://doi:10.22506/ti/2018/v25/i1/21569.
3. Çevik UA, Sağlık BN, Korkut B, Özkay Y, Ilgın S. Antiproliferative, cytotoxic, and apoptotic effects of new benzimidazole derivatives bearing hydrazone moiety. J Heterocyclic Chemistry. 2017; 55:138. https://doi:10.1002/jhet.3016.
4. Singh H, Lonare MK, Sharma M, Udehiya R, Singla S, Saini SP, Dumka VK. Interactive effect of carbendazim and imidacloprid on buffalo bone marrow derived mesenchymal stem cells: Oxidative stress, cytotoxicity and genotoxicity. Drug Chem Toxicol. 2021; 29:1-15. https://doi.org/10.1080/01480545.2021.2007023. PMID: 34844488.
5. Caron-Beaudoin E, Viau R, Hudon-Thibeault AA, Vaillancourt C, Sanderson JT. The use of a unique co-culture model of fetoplacental steroidogenesis as a screening tool for endocrine disruptors: The effects of neonicotinoids on aromatase activity and hormone production. Toxicol Appl Pharmacol. 2017; 332:15-24. https://doi.org/10.1016/j.taap.2017.07.018. PMID: 28750898.
6. Lonare M, Kumar M, Raut S, Badgujar P, Doltade S, Telang A. Evaluation of imidacloprid-induced neurotoxicity in male rats: A protective effect of curcumin. Neurochem Int. 2014; 78:122-129. https://doi.org/10.1016/j.neuint.2014.09.004. PMID: 25261201.
7. Chakroun, Intissar G, Lobna E, Oumaïma A, Fadoua N, Emna K, Najjar MF, Zohra H, Hassen BC. Imidacloprid enhances liver damage in Wistar rats: Biochemical, oxidative damage and histological Assessment. J Coastal Life Med. 2017; 5(12):540-546. https://doi.org/10.12980/jclm.5.2017J7-149.

8. Casida JE. Pesticide interactions: Mechanisms, benefits, and risks. J Agric Food Chem. 2017; 65(23):4553-4561. https://doi:10.1021/acs.jafc.7b01813.
9. Hernández AF, Gil F, Lacasaña M. Toxicological interactions of pesticide mixtures: An update. Arch Toxicol. 2017; 91(10):3211-3223. https://doi.org/10.1007/s00204-017-2043-5. PMID: 28845507.
10. Lonare MK, Vemu B, Singh AK, Dumka VK, Singla S, Sharma SK. Cytotoxicity and oxidative stress alterations induced by aldrin in BALB/c 3T3 fibroblast cells. Proc Natl Acad Sci India Sect B Biol Sci. 2017; 87:1209-1216. https://doi.org/10.1007/s40011-015-0694-7.
11. Gade NE, Pratheesh MD, Nath A, Dubey PK, Amarpal, Sharma B, Saikumar G, Taru Sharma G. Molecular and cellular characterization of buffalo bone marrow-derived mesenchymal stem cells. Reprod Domest Anim. 2013; 48(3):358-367. https://doi.org/10.1111/j.1439-0531.2012.02156.x.
12. Devi P, Sharma M, Singh SD, Lonare MK, Udehiya R. Viability and expression pattern of cryopreserved mesenchymal stem cells derived from buffalo bone marrow. Ruminant Sci. 2017; 6(1):7-12.
13. Aranda A, Sequedo L, Tolosa L, Quintas G, Burello E, Castell JV, Gombau L. Dichloro-dihydro-fluorescein diacetate (DCFH-DA) assay: a quantitative method for oxidative stress assessment of nanoparticle-treated cells. Toxicol *In Vitro.* 2013; 27(2):954-963. https://doi.org/10.1016/j.tiv.2013.01.016. PMID: 23357416.
14. Salmon ED, Shaw SL, Waters JC, Waterman-Storer CM, Maddox PS, Yeh E, Bloom K. A high-resolution multimode digital microscope system. Methods Cell Biol. 2007; 81:187-218. https://doi.org/10.1016/S0091-679X(06)81011-3. PMID: 17519169.
15. Doan CC, Truong NH, Vu NB, Nguyen TT, Nguyen HM, Nguyen KG, Do S, Phan NK, Pham PV. Isolation, culture and cryopreservation of human bone marrow derived mesenchymal stem cells. Int J Plant Animal Env Sci. 2012; 2(2):358-367.
16. Yu Y, Yao AH, Chen N, Pu LY, Fan Y, Lv L, Sun BC, Li GQ, Wang XH. Mesenchymal stem cells over-expressing hepatocyte growth factor improve small-for-size liver grafts regeneration. Mol Ther. 2007; 15(7):1382-1389. https://doi.org/10.1038/sj.mt.6300202. PMID: 17519892.
17. de Macedo Braga LM, Lacchini S, Schaan BD, Rodrigues B, Rosa K, De Angelis K, Borges LF, Irigoyen MC, Nardi NB. In situ delivery of bone marrow cells and mesenchymal stem cells improves cardiovascular function in hypertensive rats submitted to myocardial infarction. J Biomed Sci. 2008; 15(3):365-374. https://doi.org/10.1007/s11373-008-9237-z. PMID: 18256904.
18. Peterbauer-Scherb A, van Griensven M, Meinl A, Gabriel C, Redl H, Wolbank S. Isolation of pig bone marrow mesenchymal stem cells suitable for one-step procedures in chondrogenic regeneration. J Tissue Eng Regen Med. 2010; 4(6):485-490. https://doi.org/10.1002/term.262. PMID: 20112279.
19. McCarty RC, Gronthos S, Zannettino AC, Foster BK, Xian CJ. Characterisation and developmental potential of ovine bone marrow derived mesenchymal stem cells. J Cell Physiol. 2009; 219(2):324-333. https://doi.org/10.1002/jcp.21670. PMID: 19115243.
20. Rentsch C, Hess R, Rentsch B, Hofmann A, Manthey S, Scharnweber D, Biewener A, Zwipp H. Ovine bone marrow mesenchymal stem cells: isolation and characterization of the cells and their osteogenic differentiation potential on embroidered and surface-modified polycaprolactone-co-lactide scaffolds. *In Vitro* Cell Dev Biol Anim. 2010; 46(7):624-634. https://doi.org/10.1007/s11626-010-9316-0. PMID: 20490706.
21. Honda H, Tomizawa M, Casida JE. Neo-nicotinoid metabolic activation and inactivation established with coupled nicotinic receptor-CYP3A4 and -aldehyde oxidase systems. Toxicol Lett. 2006; 161(2):108-114. https://doi.org/10.1016/j.toxlet.2005.08.004. PMID: 16153789.
22. Tomizawa M, Lee DL, Casida JE. Neonicotinoid insecticides: molecular features conferring selectivity for insect versus mammalian nicotinic receptors. J Agric Food Chem. 2000; 48(12):6016-6024. https://doi.org/10.1021/jf000873c. PMID: 11312774.
23. Abolaji AO, Awogbindin IO, Adedara IA, Farombi EO. Insecticide chlorpyrifos and fungicide carbendazim, common food contaminants mixture, induce hepatic, renal, and splenic oxidative damage in female rats. Hum Exp Toxicol. 2017; 36(5):483-493. https://doi.org/10.1177/0960327116652459. PMID: 27268782.
24. Chauhan LK, Varshney M, Pandey V, Sharma P, Verma VK, Kumar P, Goel SK. ROS-dependent genotoxicity, cell cycle perturbations and apoptosis in mouse bone marrow cells exposed to formulated mixture of cypermethrin and chlorpyrifos. Mutagenesis. 2016; 31(6):635-642. https://doi.org/10.1093/mutage/gew031. PMID: 27470700.
25. Abhishek A, Ansari NG, Shankhwar SN, Jain A, Singh V. *In vitro* toxicity evaluation of low doses of pesticides in individual and mixed condition on human keratinocyte cell line. Bioinformation. 2014; 31;10(12):716-720. https://doi.org/10.6026/97320630010716. PMID: 25670872.
26. Sands M, Kron MA, Brown RB. Pentamidine: a review. Rev Infect Dis. 1985; 7(5):625-634. https://doi.org/10.1093/clinids/7.5.625. PMID: 3903942.

27. Vercesi AE, Docampo R. Ca^{2+} transport by digitonin-permeabilized Leishmania donovani. Effects of Ca^{2+}, pentamidine and WR-6026 on mitochondrial membrane potential in situ. Biochem J. 1992; 284 (Pt 2)(Pt 2):463-467. https://doi.org/10.1042/bj2840463. PMID: 1376113.
28. Andréo R, Regasini LO, Petrônio MS, Chiari-Andréo BG, Tansini A, Silva DH, Cicarelli RM. Toxicity and Loss of Mitochondrial Membrane Potential Induced by Alkyl Gallates in Trypanosoma cruzi. Int Sch Res Notices. 2015; 2015:924670. https://doi:10.1155/2015/924670. PMID: 27347554.
29. Sakamuru S, Attene-Ramos MS, Xia M. Mitochondrial Membrane Potential Assay. Methods Mol Biol. 2016; 1473:17-22. https://doi.org/10.1007/978-1-4939-6346-1_2. PMID: 27518619.
30. Area-Gomez E, Del Carmen Lara Castillo M, Tambini MD, Guardia-Laguarta C, de Groof AJ, Madra M, Ikenouchi J, Umeda M, Bird TD, Sturley SL, Schon EA. Upregulated function of mitochondria-associated ER membranes in Alzheimer disease. EMBO J. 2012; 5; 31(21):4106-4123. https://doi.org/10.1038/emboj.2012.202. PMID: 22892566.
31. Adachi M, Ishii H. Role of mitochondria in alcoholic liver injury. Free Radic Biol Med. 2002; 32(6):487-491. https://doi.org/10.1016/s0891-5849(02)00740-2. PMID: 11958949.
32. Campisi J. Aging, cellular senescence, and cancer. Annu Rev Physiol. 2013; 75:685-705. https://doi.org/10.1146/annurev-physiol-030212-183653. PMID: 23140366.
33. Shahini A, Choudhury D, Asmani M, Zhao R, Lei P, Andreadis ST. NANOG restores the impaired myogenic differentiation potential of skeletal myoblasts after multiple population doublings. Stem Cell Res. 2018; 26:55-66. https://doi.org/10.1016/j.scr.2017.11.018. PMID: 29245050.
34. Baker DJ, Childs BG, Durik M, Wijers ME, Sieben CJ, Zhong J, Saltness RA, Jeganathan KB, Verzosa GC, Pezeshki A, Khazaie K, Miller JD, van Deursen JM. Naturally occurring p16(Ink4a)-positive cells shorten healthy lifespan. Nature. 2016; 530(7589):184-189. https://doi.org/10.1038/nature16932. PMID: 26840489.
35. Bernstein H, Payne CM, Bernstein C, Garewal H, Dvorak K. Cancer and Aging as Consequences of Un-Repaired DNA Damage. New Research on DNA Damages. New York, USA: Nova Science Publishers; 2008. p.1-47.
36. Pan MR, Li K, Lin SY, Hung WC. Connecting the dots: From DNA damage and repair to Aging. Int J Mol Sci. 2016; 17(5):685. https://doi.org/10.3390/ijms17050685. PMID: 27164092.
37. Menon R, Boldogh I, Urrabaz-Garza R, Polettini J, Syed TA, Saade GR, Papaconstantinou J, Taylor RN. Senescence of primary amniotic cells via oxidative DNA damage. PLoS One. 2013; 8(12):e83416. https://doi.org/10.1371/journal.pone.0083416. PMID: 24386195.